Manuscript

Click here to access/download;Manuscript;Final manuscript reviewer changes2.docx

Click here to view linked References

A high-throughput delayed fluorescence method reveals underlying differences in the control of circadian rhythms in *Triticum aestivum* and *Brassica napus*

Hannah Rees[1,2], Susan Duncan[1], Peter Gould[2], Rachel Wells[3], Mark Greenwood[4,5], Thomas Brabbs[1], Anthony Hall[1*]

[1]Earlham Institute, Norwich Research Park, Norwich, NR4 7UG, UK

[2]Institute of Integrative Biology, University of Liverpool, Crown Street, Liverpool, L69 7ZB, UK

[3]John Innes Centre, Norwich Research Park, Norwich NR4 7UH, UK

[4]Sainsbury Laboratory, University of Cambridge, Cambridge, CB2 1LR, UK

[5]Department of Biochemistry, University of Cambridge, Cambridge, CB2 1QW, UK

Email

Anthony Hall (corresponding) anthony.hall@earlham.ac.uk*

Hannah Rees: hannah.rees@earlham.ac.uk

Susan Duncan: susan.duncan@earlham.ac.uk

Peter Gould: peter.gould@liverpool.ac.uk

Rachel Wells: rachel.wells@jic.ac.uk

Mark Greenwood: mark.greenwood@slcu.cam.ac.uk

Thomas Brabbs: thomas.brabbs@earlham.ac.uk

List of Abbreviations:

DF: Delayed Fluorescence

FFT-NLLS: Fast Fourier Transform Non-Linear Least Squares

RAE: Relative Amplitude Error

PSII: Photosystem II

L:L: Constant light

L:D: Light-dark cycles

D:D: Constant Dark

BnDFFS: *Brassica napus* Diversity Fixed Foundation Set

ZT: Zeitgeber time

Baseline and amplitude (BAMP)

CV: coefficient of variation

Abstract

Background

A robust circadian clock has been implicated in plant resilience, resource-use efficiency, competitive growth and yield. A huge number of physiological processes are under circadian control in plants including: responses to biotic and abiotic stresses; flowering time; plant metabolism; and mineral uptake. Understanding how the clock functions in crops such as *Triticum aestivum* (bread wheat) and *Brassica napus* (oilseed rape) therefore has great agricultural potential. Delayed fluorescence (DF) imaging has been shown to be applicable to a wide range of plant species and requires no genetic transformation. Although DF has been used to measure period length of both mutants and wild ecotypes of *Arabidopsis*, this assay has never been systematically optimised for crop plants. The physical size of both *B. napus* and *T. aestivum* led us to develop a representative sampling strategy which enables high-throughput imaging of these crops.

Results

In this study, we describe the plant-specific optimisation of DF imaging to obtain reliable circadian phenotypes with the robustness and reproducibility to detect diverging periods between cultivars of the same species. We find that the age of plant material, light regime and temperature conditions all significantly effect DF rhythms and describe the optimal conditions for measuring robust rhythms in each species. We also show that sections of leaf can be used to obtain period estimates with improved throughput for larger sample size experiments.

Conclusions

We present an optimized protocol for high-throughput phenotyping of circadian period specific to two economically valuable crop plants. Application of this method revealed significant differences between the periods of several widely grown elite cultivars. This method also identified intriguing differential responses of circadian rhythms in *T. aestivum* compared to *B. napus*; specifically the dramatic change to rhythm robustness when plants were imaged under constant light versus constant darkness. This points towards diverging networks underlying circadian control in these two species.

Keywords: Circadian period, delayed fluorescence, free-running conditions, Hexaploid wheat, oilseed rape, aging, L:L, D:D, temperature, rhythm robustness

Background

A circadian clock is an endogenous oscillator entrained by external temporal cues. Circadian control of gene expression is a ubiquitous feature which appears to have arisen independently in bacteria, fungi, plants and animals(1). Since the discovery of the first *Arabidopsis* circadian mutant in 1995(2), the significance of the circadian clock in plants has become increasingly evident. Approximately 30% of genes in *Arabidopsis* are predicted to be under circadian control, regulating photosynthetic, metabolic and developmental pathways(3,4). Moreover, a selective advantage resulting from a clock which is matched to the exogenous day-length has been demonstrated in mammals, insects, bacteria and plants(5–9).

The most recent model for the molecular control of the *Arabidopsis* clock is comprised of a series of interlocking negative transcriptional feedback loops regulated by key activators which control the oscillation of clock gene expression(10). To ascertain the underlying nature of circadian rhythms, a clock-controlled output representing the pace of the clock must be measured in constant (free-running) conditions. Previously this research has been conducted by studying leaf movement rhythms or by following luciferase gene expression under the control of a circadian regulated promoter(11–13). Delayed fluorescence (DF) imaging provides an alternative to these methods that does not require plant transformation. It has previously been shown to work in a variety of plants for which leaf movement assays are not feasible(14,15). Delayed fluorescence occurs when excited electrons in photosystem II (PSII) undergo spin-conversion to a triplet excited state before charge recombination allows them to return to their ground state releasing light energy(16). Measurements of DF have been correlated with the photosynthetic state of PSII(17) and the amount of DF production is regulated by the circadian clock. DF can be measured with a low-light imaging system identical to that used for luciferase imaging and output rhythms

have been shown to oscillate with a comparable period to those estimated from luciferase reporter experiments(14). The output from a DF experiment is a waveform which has parameters that can be mathematically defined and therefore quantified. These parameters include ‘period’ (the time taken to complete one cycle), ‘phase’ (the time of day at which this peaks) and ‘amplitude’ (the distance between the peak and the baseline of the oscillation). Important to circadian dynamics is also the idea of ‘rhythm robustness’ i.e. whether these parameters change over time. In this paper, rhythm robustness was assessed by: the percentage of samples classified as rhythmic; the relative amplitude error (RAE); the period coefficient of variation (CV) and the average period error threshold (all defined in Supplementary Materials). Together, these parameters allow the effects of different imaging conditions to be quantified.

As DF measurement is correlated with the oscillations in photosynthetic status of PSII, leaf material is the logical choice for a representative sample. Rhythms have been shown to persist in excised leaves in several species(18–22). However, previous research has demonstrated that independent clocks run at different periods throughout the plant under constant conditions, coordinated by a degree of intercellular coupling(23–27). The extent to which the clock is affected by dissecting leaf material into small segments is investigated in this paper.

Alongside these spatial differences, the clock has also been shown to be temporally dynamic and is affected by the life history of the plant. Both the systemic age of the plant and the ‘emergence age’ of the individual leaves on a plant have been reported to effect the clock in *Arabidopsis*, with increasing age associated with period reduction(28). Conversely, the timing of leaf senescence has also been shown to be directly regulated by core circadian genes(29).

In addition to this endogenous entrainment, the clock is also responsive to external stimuli; the most well characterized of which are light and temperature cues. Increasing light intensity causes a shortening of period in free-running conditions(30–32) and these rhythms rapidly dampen in amplitude under continuous darkness(33). Circadian systems are relatively buffered against temperature changes compared to other biochemical reactions but are not completely independent of it(34). Period shortening of 1.8–4.2h have been reported following temperature increases from 17°C to 27°C determined by both leaf-movement assays and luciferase reporters under circadian regulation in *Arabidopsis*(31,35,36). Seedlings grown at 17°C also have rhythms with lower period variability and RAE values than plants grown at 27°C(35,37). The extent to which rhythms are temperature compensated is described using the inverse of the temperature coefficient Q10; the change in the rate of a process over a temperature change of 10°C(38).

Here we present an optimized protocol for high-throughput phenotyping of circadian period using two crop plant models; *Triticum aestivum* (bread wheat) and *Brassica napus* (oilseed rape). *B. napus* (AACC) and *T. aestivum* (AABBDD) are both recent polyploids still undergoing genomic rearrangements. The contribution of each genome to clock function remains to be investigated. *B. napus* is a dicot recently diverged from *Arabidopsis*(39) and so is likely to have clock homologs with similar functions. *T. aestivum* is a monocot with an incompletely understood clock mechanism(40). These species therefore provide interesting insights into two genetically diverse families. Both *T. aestivum* and *B. napus* have been influenced by human domestication, genome duplication events and geographical speciation as the use of these crops became globalized. The specific and combined effects of these factors on the control of the clock is yet to be investigated.

Within this paper we show that both the age of the plant and the developmental age of leaves have significant effects on period with older material displaying shorter rhythms. To make our method high-throughput whilst still providing reliable rhythms, tissues were segmented into various sizes and compared to whole leaf samples. We identify regions of the plant leaves which are the most robustly rhythmic and give the most consistent period estimates. Both the light regime and temperature conditions also had large effects on period estimation and we describe conditions optimal for each species.

Finally, we applied our optimized, high-throughput DF method to investigate differences between elite cultivars in both *B. napus* and *T. aestivum* and demonstrate it to be a useful tool for assaying circadian rhythms in these crop species.

Results

<u>Circadian variability due to leaf development and age of plant</u>

We tested the effect of both plant and leaf aging on period estimates from *Brassica* and wheat seedlings. Previous studies in *Arabidopsis* have reported that the pace of the clock increases as the plant ages and that earlier emerged leaves have a shorter period than those which emerge later within the same individual(28). Our results mirror these findings for young wheat and *Brassica* plants, however this association was lost for older material (Figure 1A). For wheat we calculated period estimates from the second leaf of plants at 18, 25, 32 and 39 days after sowing and show that between 18-32 days period decreases linearly at a rate of approximately half an hour per week while maintaining a near constant relative amplitude error (RAE) (Figure 1A and B). However, in leaves from 39 day old plants there was an increase in both average period and relative amplitude error, potentially due to metabolic changes as a leaf changes from a source to a sink tissue or due to the onset of

senescence in these samples. A one-way analysis of variance yielded a significant effect of wheat age on both period and RAE ($F(3,90)=12.13$, $p<0.001$) and ($F(3,90)=7.018$, $p<0.001$) respectively. Based on our investigation, we recommend using plants between 25 to 32 days after sowing. At 25 days 100% of samples were classified as rhythmic and period CV was 1.52h. 32 day old samples were also robust, having the lowest RAE (0.15) and period error (0.43) averages (see Supplementary Materials S1.)

In a separate experiment, we analyzed 4 leaves from 25 day old wheat plants as is shown in Figure 1C, where leaves 1 and 3 were the oldest leaves and leaves 2 and 4 the second oldest leaves from the main and secondary tiller, respectively. There was a statistically significant difference between the mean periods at each leaf age (one-way ANOVA ($F(3,83)=7.434$, $p<0.001$). Within each tiller pair, the older leaf had a shorter period than the younger leaf and had higher RAE averages (Figure 1D and E). The mean period for leaf 4 (24.50h) was found to be significantly longer than both leaf 1 (23.15h) and leaf 3 (23.32h) (Tukey HSD). We recommend using leaf 2 as it had the best overall circadian robustness with regards to the % samples returned (100%), RAE (0.18) and period error (0.50) (Supplementary Materials S2).

For *Brassica* seedlings, plants were grown to 4 different ages: 20, 25, 30 and 35 days after sowing and leaf 1, 3 and 5 were sampled in the same experiment with leaf 1 being the earliest emerged leaf and leaf 5 the most recently emerged leaf (Figure 2). We conducted a nested ANOVA to test the effects of both plant age and within-plant leaf-age on period. We found that variation in plant-age had a significant effect on period, with increasing age causing a shortening of period ($F(3, 53)=8.48$, $p<0.001$). The nested effect of leaf age within each plant age-group was also found to be significant ($F(8, 53)=5.45$, $p<0.001$). The largest difference between leaves in each age-group was seen for 20 day old plants where a

difference of 3.14h was observed between leaf 1 and 5 ($p<0.001$, Tukey HSD) (Figure 2A). Brassica plant-age was also found to have a significant effect on RAE averages with younger plants having a lower mean RAE ($F(3,53)=5.953$, $p<0.01$) (Figure 2B). Supplementary Materials S3 shows robustness statistics for all plant ages and leaf-ages tested. We recommend using leaf 1 from 20 day old plants as they had the lowest RAE (0.15) and period error threshold (0.47).

To approximate the period shortening due to plant aging in *Brassica* we followed the changes in average period in leaf 5 across plant ages from 20 days after sowing to 30 days after sowing. Our analysis revealed that period shortened by approximately 3 hours per week from a mean of 26.50h(SD 1.17) to 22.38h (SD 0.62).

<u>Finding an optimal size of leaf sample</u>

We needed to identify representative leaf sections which allowed a sufficient number of samples to be analyzed on one plate without compromising the robustness of rhythms for period estimation. For wheat, we selected leaf 2 from 25 day old plants and analyzed the periods and circadian robustness given by whole leaves compared to leaves cut into 10cm sections and leaves cut into 4cm sections as shown in Figure 3A. By taking 4cm samples from 2 regions on the same leaf (5 or 15cm down from the tip) we could investigate changes in period across the length of the leaf. For *Brassica* seedlings we selected leaf 1 from 21 day old plants and then kept them whole, took 3cm square samples from the centre or quartered them (Figure 3B). This helped inform whether any changes in circadian characteristics were a result of size reduction or from sub-sectioning regions of the leaf. Our data showed that period and RAE averages were not significantly affected by cutting samples in wheat (Figure 3C and 3D), ($F(3,75)= 2.066$, $p>0.1$, one-way ANOVA). However,

cutting *Brassica* leaves did significantly affect period estimates; quartered segments had a slightly longer period than whole samples (F(2,113)=5.46, $p<0.01$, one-way ANOVA, Tukey HSD (Whole-Quarter $p<0.01$) but RAE means were similar (Figure 3E and 3F) (Supplementary Materials S4). From this data we recommend using 10cm segments for wheat and 3cm square sections for *Brassica* imaging as these gave similar results to whole leaves and increased throughput by 44% for *Brassica* and 100% for wheat.

We next wanted to investigate whether period estimates changed across the axis of the leaf. We selected only the whole leaf images and digitally sectioned them into 10 or 5 regions of interest for wheat and *Brassica* leaves respectively (Figure 3G and 3H). Using this approach we observed an average within-leaf variance of 0.45h in wheat and 0.42h in *Brassica* leaves. This variation was larger than the leaf-to-leaf variation determined for wheat (0.04h) and *Brassica* (0.3h) leaves. The mean period and RAE for each section across these leaves was calculated and plotted (Figure 3G and 3H). No significant difference was observed between the period of wheat or *Brassica* segments; however the RAE was significantly different across wheat leaves (F(9,139)=6.077, $p<0.001$, One-way ANOVA). The middle segments (4, 5, 6, 7 and 8) had significantly lower RAE averages compared to the tip (segment 1) suggesting that this middle region may give the most robust DF rhythms.

<u>Constant free-running conditions: Dark versus Light</u>

Two light regimes were tested which allowed free-running DF rhythms to be recorded. We entrained plants for 4 days in 12:12 light:dark (L:D) cycles at 22°C before sampling and imaging every hour under constant conditions, as described in Figure 4A. In both D:D and L:L conditions the exposure time was kept at 1 minute. Figure 4B shows the striking differences in period estimate accuracy obtained from wheat and *Brassica* under the two light regimes.

For wheat, periods from leaves under a D:D regime had much lower variance than those under the L:L regime (D:D mean =23.29h, SD=0.53; L:L mean =23.54h, SD=3.19). For *Brassica* the opposite was observed; rhythms were more accurate under L:L (D:D mean=24.89h, SD=2.91; L:L mean=22.92h, SD=0.31). A shortening of period was observed for both *Brassica* and wheat under L:L compared to D:D based on median values, however the increased variance observed within wheat-L:L and *Brassica*-D:D resulted in these differences having low significance (wheat t(23.16)=-0.38, p>0.5; *Brassica* t(10.14)=2.24, p=0.048 Welch's t-test).

RAE ratios reflected the accuracy seen in period estimation between the regimes (Figure 4C). RAE averages were smaller in D:D for wheat (D:D mean=0.20, SD=0.08; L:L mean=0.38, SD=0.18) and in L:L for *Brassica* (D:D mean=0.53, SD=0.13; L:L mean=0.13, SD=0.02). RAE differences were significant between regimes for both species (Wheat t(29.23)=-4.38, p<0.001; *Brassica* t(10.39)=9.92, p<0.001 Welch's t-test). Figure 4D and E show mean oscillation traces which demonstrate how DF rhythms were sustained in wheat and *Brassica* under the different light conditions. Interestingly, DF rhythms also had a dawn-phased peak in wheat and a dusk-phased peak in *Brassica* which became shifted as different light conditions were applied (Figure 4F).

Wheat samples under the D:D conditions returned 100% of samples from period estimation (L:L=95.83%), an average RAE ratio of 0.20 (L:L=0.38), a period CV of 2.25% (L:L=13.53%) and a period error threshold of 0.55 (L:L=1.17). For *Brassica*, rhythms under the L:L regime returned 100% from period estimation (D:D=66.67%), a RAE average of 0.13 (D:D=0.53), a period CV of 1.34% (D:D= 11.80) and a period error threshold of 0.41 (D:D=1.62). See Supplementary Materials S5. We would therefore recommend running wheat DF experiments under D:D conditions and *Brassica* DF experiments under L:L.

Finding an optimum free-running temperature

To investigate the effect of temperature on period and rhythm robustness we tested *Brassica* and wheat seedlings at a range of constant temperatures. We used the optimal conditions from the variables so far tested and entrained each batch of plants at the imaging temperature for four days prior to imaging (see Methods). Both *Brassica* and wheat experienced an acceleration of the clock at higher temperatures, with the rate increasing most dramatically at lower temperatures (Figure 5A). Periods decreased from 26.40h (SD=3.60) at 17°C to 22.48h (SD=0.31) at 32°C in wheat. Periods decreased from 26.28h (SD=0.72) at 12°C to 23.16h (SD=0.52) at 22°C in *Brassica*. The temperature coefficient Q10 was calculated as an average across all temperatures (Supplementary Materials S7). Q10 was found to be 1.12 for wheat and 1.14 for *Brassica* indicating a degree of thermal compensation, but to a lesser extent than has been previously reported in *Arabidopsis* (36). We next looked at which temperatures gave the best rhythmicity in each crop. Rhythms were most robust in wheat grown at 27°C: 100% of period estimates were returned, the average RAE ratio was 0.15, period CV was 2.48% and period error threshold was 0.48 (Supplementary S6). There was a clear negative trend in period CV as the temperature increased in wheat from 13.63% at 17°C to 1.38% at 32°C. Mean RAE at each temperature can be seen in Figure 5B.

Across the temperatures tested *Brassica* rhythm robustness remained consistent; all samples were returned from FFT-NLLS and RAE, period CV and Period error were similar (Figure 5B, Supplementary Materials S6). We recommend 22°C for DF using *Brassica* as it had the lowest period CV of 2.24%.

288

289 <u>An optimized DF method can be used in circadian analysis for crops</u>

290 To see whether the optimized method could be used to investigate circadian differences

291 between cultivars of the same species, we looked at circadian rhythms from seven *T.*

292 *aestivum* cultivars and three *B. napus* cultivars. For the *B. napus* lines, seeds were obtained

293 from 3 different harvest years to see whether period was constant between batches. The

294 optimized imaging parameters we used for these elite cultivars is outlined in Table 1

295

Species	**Plant age** (days after sowing)	**Leaf age** (1=oldest leaf)	**Cut sample**	**Light regime**	**Temperature**	**Throughput** (N/imaging cabinet)	**% return** (from period estimation algorithms)
Brassica	20	1	3cm square	L:L	22°C	36	96.3
Wheat	25	2	10cm section	D:D	27°C	44-48	98.8

Table 1. Optimised DF method for circadian phenotyping of *Brassica* and wheat leaves

296

297 There was significant variation in the periods of the wheat lines tested as shown in Figure

298 6A ($F(6,152)=9.81$, $p<0.001$, one-way ANOVA). A Tukey HSD test showed that Paragon

299 (mean=23.48h, SD=0.54) and Norin 61 (mean=23.50h, SD=1.30) both have longer periods

300 than Chinese Spring (mean=22.70h, SD=0.40), Claire (mean=22.48, SD=0.54) and Robigus

301 (mean=22.32h, SD=0.34) $\alpha=0.01$).

302 Figure 6B shows the variation in period across three *Brassica* lines taken from three seed

303 batches. We conducted a two-way analysis of variance to compare cultivar ID and seed

304 batch effects as well as the interaction between the two factors. The cultivar ID was found

305 to have a significant effect on period ($F(2,60)=25.47$, $p<0.001$) but batch year did not

306 significantly account for any variation in period either as a main effect ($F(2,60)=1.73$, $p>0.1$)

307 or as an interaction with the cultivar ID ($F(4,60)=2.27$, $p=0.72$). This suggests that the

observed differences in period are due to heritable genetic differences. The *Brassica* cultivar Norin had the shortest overall period of 22.29h (SD 0.34); shorter than either Cabriolet (23.32h, SD=0.57) or Chuanyou II (23.18h, SD=0.72) (p<0.001, Tukey HSD).

DF oscillations in both *Brassica* and wheat remained rhythmic throughout the experiment allowing confident period estimation over 4 days (24-120h following T_0). The average DF oscillations for the two most divergent wheat lines is shown in Figure 6C; the other lines have been omitted for clarity. DF expression from all three years was averaged to make the oscillation plots for the *Brassica* lines as shown in Figure 6D. The percentage of DF rhythms returned from period estimation was high for both *Brassica* (96.3%) and wheat (98.8%) proving that the method is both efficient and reliable.

The overall throughput of this assay is dependent on the expected exclusion rate from period analysis and on the number of imaging cabinets available. Designs with 3 replicates per plate allow 10 independent lines to be assayed per cabinet over one experiment allowing for an expected 5% loss of samples. If rhythms are expected to be less robust, for example in a mutant screen, we suggest using a larger number of replicates. The scaling-up of this imaging assay to multiple cabinets is also becoming increasingly affordable as the CCD camera technology progresses.

Discussion

Manipulating the circadian clock has potential for influencing crop productivity, efficiency and resilience; however research has been hindered by the lack of high-throughput circadian protocols which can be reliably applied to crop plants. Transcriptional assays, luciferase constructs and fluorescent markers have been used to investigate circadian rhythms in tobacco(13), tomato(41), potato(42,43), *Brassica rapa*(44), rice(45–47),

barley(48) and wheat(49). However, these approaches are either manually intensive, technologically expensive or require genetic modification to systematically investigate each component and so are low throughput. We have optimized a delayed fluorescence imaging method for reliable circadian phenotyping of either *Brassica* or wheat seedlings. Several differences between the function of these clocks have been exposed through the factors examined in this paper. The opposing robustness of clocks under D:D or L:L and the fact that DF rhythms peak with distinct phases under each condition is indicative of diverging networks underlying circadian control of each species. Lower temperatures (17°C) also seem to have a detrimental effect on the robustness of the clock in *T. aestivum* but not *B. napus*, suggesting that temperature may be a stronger zeitgeber for wheat than for *Brassica* within this temperature range. The DF rhythms in both *T. aestivum* and *B. napus* have reduced temperature compensation compared to those reported for leaf movement in *Arabidopsis*(36,37). However, it is important to recognize that our rhythms were measured in dissected sections of leaves and may not be truly analogous to rhythms from whole *Arabidopsis* individuals. The difference between intact and excised leaves has been previously reported in Hall et al. 2001(22). Our analysis of the homogeneity of periods across a single leaf also revealed variability of period robustness across the axis of wheat leaves but relatively little variation across *Brassica* leaves.

In this study, we have shown that in both *Brassica* and wheat there is a strong interaction between circadian period and age due to both systemic aging and leaf-specific developmental aging. Previous research in *Arabidopsis* has asked whether the onset of senescence is a result of a faster running clock or vice versa(28,50). Our results suggest that the acceleration of the clock occurs in very young plants before senescence phase, raising

the possibility that the clock could be artificially manipulated to moderate senescence and control timing of peak productivity in crops.

Natural variation of circadian phenotypes has been previously demonstrated in wild *Arabidopsis* accessions (35,36,51) revealing a selection pressure for circadian traits specific to different ecological settings. The extent to which circadian fitness has been selected-for in modern crop plants has not yet been investigated. Application of our optimized protocol in this study demonstrates that diverging rhythms are present within elite cultivars of the same species. This variation in circadian period suggests that some level of circadian diversity exists, but the question remains as to whether each cultivar is currently optimized to enhance individual plant fitness. Crop plants with 'optimized circadian clocks' may have the capacity to improve yield, efficiency and resilience potentially overlooked by traditional plant breeding methods.

Conclusions

In this study, we investigated several important factors influencing circadian rhythms in *Brassica napus* and *Triticum aestivum* and reveal intriguing differences between the two crops. We provide an optimized DF methodology which can be reliably used for high-throughput measurement of circadian rhythms. This research highlights the considerable plasticity of the circadian clock under free-running conditions. It is our hope that these results may inform future research by showing the extent to which controllable variables can affect period estimation and how these may differ depending on the model species being studied.

Method

Plant material and growth conditions

Brassica seedlings used were from the winter varieties Cabriolet and Norin and the semi-winter variety Chuanyou II from the OREGIN *Brassica napus* Diversity Fixed Foundation Set (BnDFFS)(52). Wheat seedlings used were all hexaploid elite cultivars ordered from the Genome Resource Unit (John Innes Centre) (Supplementary Materials S8).

Brassica plants were grown in Levington's F2 mix in FP11 pots, spaced 5 plants to a pot. They were grown in controlled greenhouse conditions, (16:8h L:D at 22:20°C). After 17 days, plants were transferred to a plant growth chamber set at 12:12 L:D cycle at 22°C under approximately 200µmol m^{-2} s^{-1} white light for 4 days entrainment (light spectra can be seen in Supplementary Materials S9).

Wheat plants were imbibed at 4°C for 6 days before being planted in Petersfield cereal mix in FP9 pots, spaced two to a pot. They were then grown in controlled greenhouse conditions (16:8h L:D 17:12°C). After 21 days plants were transferred to a plant growth chamber set at the cabinet conditions above. For temperature experiments, plants were entrained at the temperatures in which they would be imaged.

Image acquisition-standard conditions

Leaves were removed just after entrainment dawn and placed face up onto 24cm square petri dishes (Stratlab LTD, cat no. 163-PB-007) containing 0.5% water agar (Sigma-Aldrich, SKU A1296). Unless otherwise stated, 3cm squares were cut from the second true leaf of 21 day old *B. napus* seedlings. A segment of 10cm was taken from the second leaf of the main tiller of 25 day old *T. aestivum* seedlings, beginning 5cm down from the tip. A small strip of agar was placed over the ends of wheat sections to prevent leaf curling during the experiment. Plates were secured with masking tape around the periphery.

The imaging set-up is adapted from that described by Southern et al(53). A set-up schematic can be seen in Supplementary Materials S10. We use Lumo Reteiga CCD cameras (QImaging, Canada), which we have found to have comparable image quality to the Orca II (Hamamatsu Photonics, Japan) without the need to run a water-cooling pump. Cameras were fitted with a Xenon 0.95/25mm lens (Schneider-Kreuznach, Germany).

A custom built 25x25 red/blue LED rig (approx. 60 µmol m^{-2} s^{-1}) was controlled by µManager software (v1.4.19, Open Imaging) through an Arduino Uno microcontroller board(54). LED spectra for cabinets can be viewed in Supplementary Materials S9. µManager was used to configure both the supplied camera driver software (PVCam v3.7.1.0) and program the Arduino after installing the firmware source code available online (55)).

Both camera and LEDs were housed in a temperature controlled growth cabinet (Sanyo MIR-553) in a dark room. The temperature was set to 22°C unless otherwise specified (changed for the temperature experiments (Figure 5) and for the wheat cultivar experiment (Figure 6)). Camera properties were kept the same in each experiment (Binning=4, Gain=1, Readout-Rate=0.650195MHz 16 bit) and camera exposure was initiated 500ms after the lights were turned off. A 'L:L' script refers to a regime of 59min of light followed by a 1 minute exposure in the dark. A 'D:D' script refers to 54min of darkness followed by 5min light and then the 1min exposure. BeanShell scripts run by µManager have been adapted from scripts used previously(56) and are available to view as Additional files 15 and 16. Wheat imaging used the D:D script and *Brassica* imaging used the L:L script with the exception of experiments in Figure 4.

<u>Processing in FIJI and BioDare2 parameters</u>

Image stacks were imported into FIJI(57) and regions of interest were selected. Measurements for integrated density were taken for these regions across the stack using the Multi-measure plugin. Each region was then labeled in Excel and an offset time series added. The 'offset time' is the difference between the time of the first image (T1) and entrainment dawn (ZT) in decimal hours. Data can then be uploaded to BioDare2 as described online(58,59). BioDare2 is an open-access web tool for analyzing timeseries data and predicting circadian parameters. For our data we found that Baseline and amplitude (BAMP) de-trending was most appropriate but recommend visual inspection of the detrending methods available to find the least intrusive method which removes any baseline trends. Period estimation was done using the Fast Fourier Transform Non-Linear Least Squares (FFT-NLLS) algorithm(60) on a data window of 24-120h with expected periods set to 18-34h. Manual inspection of resulting periods ensured that all arrhythmic traces were excluded from further analysis.

Rhythm Robustness analysis

We summarized rhythm robustness metrics based on several BioDare2 outputs. '% returned' is the number of samples for which periods could be estimated out of the number of samples originally imaged. The RAE (relative amplitude error) is the ratio of amplitude error to amplitude and represents amplitude robustness. A RAE of 1 indicates the most irregular waveform which can still be classified as rythmic whereas a RAE of 0 indicates a perfect sine wave with no amplitude error. The period coefficient of variation (CV) is the standard deviation of period estimates adjusted for the mean period and represents between sample variation(58,61). Period error is the extent to which the period estimate could vary and still give a good fit to the model. Error scores close to 0 indicate a tight fit of

the model to the observed data and a high within sample period robustness. See Supplementary data S1-6 for statistic tables and further descriptions.

Normalization for experimental effects

After circadian parameters were estimated in BioDare2, data was normalized to account for the following random experimental effects. For the wheat plant age and leaf age experiments (Figure 1), *Brassica* plant-leaf age experiments (Figure 2) and the *Brassica* cultivar experiments (Figure 6B) samples were split between two imaging cabinets run in parallel in a single experiment. The predicted parameters (e.g. period) for each sample from the two cabinets were adjusted so that the cabinet means were then equivalent. This was achieved by dividing the cabinet means by the overall mean to get an adjustment factor for each cabinet and then dividing each individual value by that factor to get a cabinet-normalized value. For the cutting data (Figure 3), the experiments were replicated in two separate imaging weeks and then adjusted for the between-experiment effects. For the wheat cultivar experiments (Figure 6A) data was obtained from two cabinets over two separate experiments and was normalized for both effects in a similar way. The light regime (Figure 4) and the temperature experiments (Figure 5) measured each variable in one cabinet at a time and therefore did not require any normalization. The conclusions from these experiments is consistent with preliminary experiments presented in Supplementary Materials S11-14.

Statistical analysis was carried out in RStudio v1.1.423 using aov and t.test functions fit with an appropriate linear model in the format specified in the Results.

Declarations

Ethics approval and consent to participate

Not applicable

Consent for publication

Not applicable

Availability of data and materials

The datasets generated during the current study are available as additional files and supplementary materials in the online version of this article. Raw image files are available from the corresponding author on reasonable request.

Competing interests

The authors declare that they have no competing interests.

Funding

This project was supported by the BBSRC via the Earlham institute CSP (BB/P016774/1, AH SD, HR) and BBSRC Design Future Wheat (BB/P016855/1, AH)

Authors' contributions

This project was conceptualized by HR and AH. HR designed and conducted experiments, carried out data processing and analysis and wrote the manuscript with contributions from AH. All authors read and approved the final manuscript.

Abbreviations: Hannah Rees (HR), Susan Duncan (SD), Peter Gould (PG), Rachel Wells (RW), Mark Greenwood (MG), Thomas Brabbs (TB), Anthony Hall (AH)

References

1. Young MW, Kay SA. Time zones: a comparative genetics of circadian clocks. Nat Rev Genet. 2001 Sep 1;2(9):702–15.

2. Millar AJ, Straume M, Chory J, Chua NH, Kay SA. The regulation of circadian period by phototransduction pathways in Arabidopsis. Science. 1995 Feb 24;267(5201):1163–6.

3. Harmer SL, Hogenesch JB, Straume M, Chang HS, Han B, Zhu T, et al. Orchestrated transcription of key pathways in Arabidopsis by the circadian clock. Science. 2000 Dec 15;290(5499):2110–3.

4. Covington MF, Maloof JN, Straume M, Kay SA, Harmer SL. Global transcriptome analysis reveals circadian regulation of key pathways in plant growth and development. Genome Biol. 2008;9(8):R130.

5. Dodd AN, Salathia N, Hall A, Kévei E, Tóth R, Nagy F, et al. Plant circadian clocks increase photosynthesis, growth, survival, and competitive advantage. Science. 2005;309(5734):630–3.

6. Ouyang Y, Andersson CR, Kondo T, Golden SS, Johnson CH. Resonating circadian clocks enhance fitness in cyanobacteria. Proc Natl Acad Sci U S A. 1998 Jul 21;95(15):8660–4.

7. DeCoursey PJ, Walker JK, Smith SA. A circadian pacemaker in free-living chipmunks: essential for survival? J Comp Physiol A. 2000 Feb;186(2):169–80.

8. von Saint Paul U, Aschoff J. Longevity among blowfliesPhormia terraenovae R.D. kept in non-24-hour light-dark cycles. J Comp Physiol. 1978 Sep;127(3):191–5.

9. Pittendrigh CS, Minis DH. Circadian systems: longevity as a function of circadian resonance in Drosophila melanogaster. Proc Natl Acad Sci U S A. 1972 Jun;69(6):1537–9.

10. Hernando CE, Romanowski A, Yanovsky MJ. Transcriptional and post-transcriptional

control of the plant circadian gene regulatory network. Vol. 1860, Biochimica et Biophysica Acta - Gene Regulatory Mechanisms. 2017. p. 84–94.

11. Edwards KD, Millar AJ. Analysis of Circadian Leaf Movement Rhythms in Arabidopsis thaliana. In: Rosato E, editor. Circadian Rhythms: Methods and Protocols. Totowa, NJ: Humana Press; 2007. p. 103–13.

12. Welsh DK, Imaizumi T, Kay SA. Real-Time Reporting of Circadian-Regulated Gene Expression by Luciferase Imaging in Plants and Mammalian Cells. In: Methods in enzymology. 2005. p. 269–88.

13. Millar AJ, Short SR, Chua N-H, Kay SA. A novel circadian phenotype based on firefly luciferase expression in transgenic plants. Plant Cell. 1992;4(9):1075–87.

14. Gould PD, Diaz P, Hogben C, Kusakina J, Salem R, Hartwell J, et al. Delayed fluorescence as a universal tool for the measurement of circadian rhythms in higher plants. Plant J. 2009 Jun;58(5):893–901.

15. Gawroński P, Ariyadasa R, Himmelbach A, Poursarebani N, Kilian B, Stein N, et al. A distorted circadian clock causes early flowering and temperature-dependent variation in spike development in the Eps-3Am mutant of einkorn wheat. Genetics. 2014 Apr;196(4):1253–61.

16. Goltsev V, Zaharieva I, Chernev P, Strasser RJ. Delayed fluorescence in photosynthesis. Photosynth Res. 2009 Sep 23;101(2–3):217–32.

17. Kurzbaum E, Eckert W, Yacobi YZ. Delayed fluorescence as a direct indicator of diurnal variation in quantum and radiant energy utilization efficiencies of phytoplankton. Photosynthetica. 2007 Dec;45(4):562–7.

18. Gould PD, Diaz P, Hogben C, Kusakina J, Salem R, Hartwell J, et al. Delayed fluorescence as a universal tool for the measurement of circadian rhythms in higher

plants. Plant J. 2009;58(5):893–901.

19. Boxall SF, Dever L V, Kneřová J, Gould PD, Hartwell J. Phosphorylation of Phosphoenolpyruvate Carboxylase Is Essential for Maximal and Sustained Dark CO2 Fixation and Core Circadian Clock Operation in the Obligate Crassulacean Acid Metabolism Species Kalanchoë fedtschenkoi. Plant Cell. 2017 Oct 1;29(10):2519–36.

20. Thain SC, Hall A, Millar AJ. Functional independence of circadian clocks that regulate plant gene expression. Curr Biol. 2000 Aug 14;10(16):951–6.

21. Takahashi N, Hirata Y, Aihara K, Mas P. A Hierarchical Multi-oscillator Network Orchestrates the Arabidopsis Circadian System. Cell. 2015 Sep 24;163(1):148–59.

22. Hall A, Kozma-Bognár L, Tóth R, Nagy F, Millar AJ. Conditional circadian regulation of PHYTOCHROME A gene expression. Plant Physiol. 2001 Dec;127(4):1808–18.

23. Endo M, Shimizu H, Nohales MA, Araki T, Kay SA. Tissue-specific clocks in Arabidopsis show asymmetric coupling. Nature. 2014 Nov 20;515(7527):419–22.

24. Thain SC, Murtas G, Lynn JR, McGrath RB, Millar AJ. The circadian clock that controls gene expression in Arabidopsis is tissue specific. Plant Physiol. 2002;130(1):102–10.

25. James AB, Monreal JA, Nimmo GA, Kelly CL, Herzyk P, Jenkins GI, et al. The circadian clock in Arabidopsis roots is a simplified slave version of the clock in shoots. Science. 2008 Dec 19;322(5909):1832–5.

26. Gould PD, Domijan M, Greenwood M, Tokuda IT, Rees H, Kozma-Bognar L, et al. Coordination of robust single cell rhythms in the Arabidopsis circadian clock via spatial waves of gene expression. Elife. 2018 Apr 26;7:e31700.

27. Wenden B, Toner DLK, Hodge SK, Grima R, Millar AJ. Spontaneous spatiotemporal waves of gene expression from biological clocks in the leaf. Proc Natl Acad Sci U S A. 2012 Apr 24;109(17):6757–62.

28. Kim H, Kim Y, Yeom M, Lim J, Nam HG. Age-associated circadian period changes in Arabidopsis leaves. J Exp Bot. 2016;67(9):2665–73.

29. Kim H, Kim HJ, Vu QT, Jung S, McClung CR, Hong S, et al. Circadian control of *ORE1* by PRR9 positively regulates leaf senescence in *Arabidopsis*. Proc Natl Acad Sci. 2018;201722407.

30. Harris PJC, Wilkins MB. Light-induced changes in the period of the circadian rhythm of carbon dioxide output in Bryophyllum leaves. Planta. 1976;129(3):253–8.

31. Somers DE, Webb AA, Pearson M, Kay SA. The short-period mutant, toc1-1, alters circadian clock regulation of multiple outputs throughout development in Arabidopsis thaliana. Development. 1998 Feb;125(3):485–94.

32. Aschoff J. Circadian Rhythms: Influences of Internal and External Factors on the Period Measured in Constant Conditions1. Z Tierpsychol. 2010 Apr 26;49(3):225–49.

33. Salomé PA, Xie Q, McClung CR. Circadian timekeeping during early Arabidopsis development. Plant Physiol. 2008 Jul;147(3):1110–25.

34. Colin Pittendrigh BS, by N Harvey CE. On temperature independence in the clock-system controlling emergence Time in Drosophila. Vol. 102, Proc. Soc. Exptl. Biol. Med. 1954.

35. Kusakina J, Gould PD, Hall A. A fast circadian clock at high temperatures is a conserved feature across Arabidopsis accessions and likely to be important for vegetative yield. Plant Cell Environ. 2014 Feb;37(2):327–40.

36. Edwards KD, Lynn JR, Gyula P, Nagy F, Millar AJ. Natural allelic variation in the temperature-compensation mechanisms of the Arabidopsis thaliana circadian clock. Genetics. 2005;170(1):387–400.

37. Gould PD, Locke JCW, Larue C, Southern MM, Davis SJ, Hanano S, et al. The Molecular

Basis of Temperature Compensation in the Arabidopsis Circadian Clock. Plant Cell. 2006 May 1;18(5):1177–87.

38. Edwards KD, Lynn JR, Gyula P, Nagy F, Millar AJ. Natural allelic variation in the temperature-compensation mechanisms of the Arabidopsis thaliana circadian clock. Genetics. 2005 May;170(1):387–400.

39. Yang Y-W, Lai K-N, Tai P-Y, Li W-H. Rates of Nucleotide Substitution in Angiosperm Mitochondrial DNA Sequences and Dates of Divergence Between Brassica and Other Angiosperm Lineages. J Mol Evol. 1999 May;48(5):597–604.

40. Campoli C, Shtaya M, Davis SJ, von Korff M. Expression conservation within the circadian clock of a monocot: natural variation at barley Ppd-H1 affects circadian expression of flowering time genes, but not clock orthologs. BMC Plant Biol. 2012 Jun 21;12:97.

41. Facella P, Lopez L, Carbone F, Galbraith DW, Giuliano G, Perrotta G. Diurnal and circadian rhythms in the tomato transcriptome and their modulation by cryptochrome photoreceptors. PLoS One. 2008 Jul 30;3(7):e2798.

42. Kloosterman B, Abelenda JA, Gomez M del MC, Oortwijn M, de Boer JM, Kowitwanich K, et al. Naturally occurring allele diversity allows potato cultivation in northern latitudes. Nature. 2013 Mar 6;495(7440):246–50.

43. Navarro C, Abelenda JA, Cruz-Oró E, Cuéllar CA, Tamaki S, Silva J, et al. Control of flowering and storage organ formation in potato by FLOWERING LOCUS T. Nature. 2011 Oct 25;478(7367):119–22.

44. Xu X, Xie Q, McClung CR. Robust circadian rhythms of gene expression in Brassica rapa tissue culture. Plant Physiol. 2010 Jun;153(2):841–50.

45. Izawa T, Mihara M, Suzuki Y, Gupta M, Itoh H, Nagano AJ, et al. Os-GIGANTEA confers

robust diurnal rhythms on the global transcriptome of rice in the field. Plant Cell. 2011 May;23(5):1741–55.

46. Sugiyama N, Izawa T, Oikawa T, Shimamoto K. Light regulation of circadian clock-controlled gene expression in rice. Plant J. 2001 Dec 23;26(6):607–15.

47. Nagano AJ, Sato Y, Mihara M, Antonio BA, Motoyama R, Itoh H, et al. Deciphering and Prediction of Transcriptome Dynamics under Fluctuating Field Conditions. Cell. 2012 Dec 7;151(6):1358–69.

48. Ford B, Deng W, Clausen J, Oliver S, Boden S, Hemming M, et al. Barley (Hordeum vulgare) circadian clock genes can respond rapidly to temperature in an EARLY FLOWERING 3-dependent manner. J Exp Bot. 2016;67(18):5517–28.

49. Beales J, Turner A, Griffiths S, Snape JW, Laurie DA. A Pseudo-Response Regulator is misexpressed in the photoperiod insensitive Ppd-D1a mutant of wheat (Triticum aestivum L.). Theor Appl Genet. 2007 Aug 24;115(5):721–33.

50. Kim H, Kim HJ, Vu T, Jung S, Robertson Mcclung C, Hong S, et al. Circadian control of ORE1 by PRR9 positively regulates leaf senescence in Arabidopsis. 2018;115(33):8448–53.

51. Michael TP, Salomé PA, Yu HJ, Spencer TR, Sharp EL, McPeek MA, et al. Enhanced Fitness Conferred by Naturally Occurring Variation in the Circadian Clock. Science (80-). 2003;302(5647):1049–53.

52. Pink D, Bailey L, McClement S, Hand P, Mathas E, Buchanan-Wollaston V, et al. Double haploids, markers and QTL analysis in vegetable brassicas. Euphytica. 2008 Nov 20;164(2):509–14.

53. Southern MM, Brown PE, Hall A. Luciferases as Reporter Genes. In: Arabidopsis Protocols. New Jersey: Humana Press; 2006. p. 293–306.

54. Arduino [Internet]. [cited 2018 Nov 14]. Available from: https://www.arduino.cc/

55. uManager-Arduino [Internet]. [cited 2018 Nov 15]. Available from: https://micro-manager.org/wiki/Arduino#Firmware

56. Litthauer S, Battle MW, Lawson T, Jones MA. Phototropins maintain robust circadian oscillation of PSII operating efficiency under blue light. Plant J. 2015 Sep 1;83(6):1034–45.

57. Schindelin J, Arganda-Carreras I, Frise E, Kaynig V, Longair M, Pietzsch T, et al. Fiji: an open-source platform for biological-image analysis. Nat Methods. 2012 Jul 1;9(7):676–82.

58. Zielinski T, Moore AM, Troup E, Halliday KJ, Millar AJ. Strengths and Limitations of Period Estimation Methods for Circadian Data. Yamazaki S, editor. PLoS One. 2014 May 8;9(5):e96462.

59. BioDare2 - circadian period analysis [Internet]. [cited 2018 Nov 14]. Available from: https://biodare2.ed.ac.uk/welcome

60. Straume M, Frasier-Cadoret SG, Johnson ML. Least-Squares Analysis of Fluorescence Data. In: Topics in Fluorescence Spectroscopy. Boston: Kluwer Academic Publishers; 1991. p. 177–240.

61. Toth R, Kevei E, Hall A, Millar AJ, Nagy F, Kozma-Bognár L. Circadian Clock-Regulated Expression of Phytochrome and Cryptochrome Genes in Arabidopsis. PLANT Physiol. 2001 Dec 1;127(4):1607–16.

Figure 1. DF rhythms in wheat change with the age of the plant and between leaves on the same plant. The wheat plant age experiment (A-B) used 'leaf 2' from plants grown for 18, 25, 32 or 39 days. Blue boxplots show differences in period (A) and RAE (B) at each plant age. The wheat leaf variation experiment used 4 leaves sampled from 25 day old plants following the leaf numbering system described in C. Orange boxplots show differences in period (D) and RAE (E) at each leaf age. Colour scales reflect an ageing gradient with lighter colours representing younger material. Data represents results from two imaging cabinets run in parallel as technical replicates and normalised for the between-cabinet effects. Period estimates were calculated using FFT-NLLS (BAMP de-trended data, 24-120h cut-off). N values reflect the number of samples for which period was estimated out of the total number of individuals sampled. Age 18 (N=26/26), age 25 (N=24/24), age 32 (N=25/26), age 39 (N=19/23). Leaf 1 (N=22/22), leaf 2 (N=22/22), leaf 3 (N=22/22), leaf 4 (N=21/22). Significance codes: ***p<0.001, **p<0.01 *p<0.05.

Figure 2. DF rhythms in *Brassica* change with the age of the plant and between different leaf ages. *Brassica* seedlings were grown to 4 different ages: 20, 25, 30 and 35 days after sowing Leaves 1, 3 and 5 were sampled from each plant in the experiment with leaf 1 being the earliest emerged leaf and leaf 5 the most recently emerged leaf. Boxplots show differences in period (A) and RAE (B) for each leaf age within each plant age. Colour scales reflect an ageing gradient with lighter colours representing younger material. Periods and RAE estimates were calculated using FFT NLLS (BAMP dtr, 24-120h cut-off). Data represents results from two imaging cabinets run in parallel as technical replicates and normalised for the between-cabinet effects. Age 20: leaf 1 (N=6/6), leaf 3 (N=6/6), leaf 5 (N=6/6). Age 25: leaf 1 (N=4/6), leaf 3 (N=6/6), leaf 5 (N=6/6). Age 30: leaf 1 (N=2/6), leaf 3 (N=5/6), leaf 5 (N=6/6). Age 35: leaf 1 (N=6/6), leaf 3 (N=6/6), leaf 5 (N=6/6). Significance codes: ***p<0.001, **p<0.01 *p<0.05, all significance markers are relative to leaf 1 at each age.

Figure 3. Cut sections of leaf material can be used to accurately make period estimates. The second leaf from 25 day old wheat seedlings was either left whole or sectioned into 10 cm or 4cm fragments cut either 5cm or 15cm from the tip (shown as dark grey sections in A). The first leaf from 21 day old *Brassica* plants was either left whole, sectioned into a 3cm square or quartered (B). Orange boxplots show differences in period (C) and RAE (D) for wheat sections. Purple boxplots show differences in period (E) and RAE (F) for brassica sections. Period and RAE were estimated using FFT NLLS, BAMP dtr, 24-120h cut-off.
Whole leaves were digitally sectioned along the axis of the leaf post image-acquisition. Wheat period and RAE means for each section are shown in G. *Brassica* period and RAE means are plotted corresponding to the sectioning shown in H. Error bars show standard deviation. Data represents results from two experiments normalised for the between-experiment effects. Wheat: Whole (N=15/15), 10cm (N=23/23), 4cm top (N=20/21), 4cm bottom (N=22/22). *Brassica*: Whole (N=20/20), Square (N=21/21), Quarter (N=75/76). Significance codes: **p<0.01.

Figure 4. Effect of either L:L or D:D free-running light conditions on DF rhythms. Wheat and *Brassica* seedlings were entrained for 4 days in L:D at 22°C before sections were cut, plated and imaged. A D:D free run consisted of a loop of 54 minutes of darkness followed by 5 minutes of light exposure and then image capture. A L:L free-run consisted of 59 minutes of light exposure before image capture (A). Boxplots of period (B) and RAE (C) are shown for *Brassica* and wheat in D:D and L:L conditions where *Brassica* data is displayed in purple

and wheat data in orange. Period and RAE were estimated using FFT NLLS, BAMP dtr, 24-120h cut-off. Examples of oscillation traces are shown in D:D (black lines) and L:L (red lines) for wheat (D) and *Brassica* (E). Thick lines represent the mean trace of 6 mean-normalised individuals with error bars representing standard deviations. Estimated individual circadian phases are shown in the clock plot in (F) where the length of the line reflects the inverse circadian phase error (longer lines imply more confidence in the phase prediction). All phase estimates are relative to 0 where 0 represents entrainment dawn and 12 represents dusk.
D:D *Brassica* (N=12/18); D:D Wheat (N=24/24); L:L *Brassica* (N=18/18); L:L Wheat (N=23/24). Data is consistent with additional preliminary experiments which can be seen in Supplementary S11 and S12. Significance codes: ***p<0.001.

Figure 5. Increasing temperature causes a shortening of period and effects rhythm robustness. Wheat and *Brassica* seedlings were entrained for 4 days in L:D at the temperature being assessed before imaging. Each temperature point represents a separate imaging experiment. Period means decrease with increasing temperatures as is shown in A for *Brassica* (purple circles) or wheat (orange triangles). Error bars represent standard deviation. Box plots show the effect of temperature on RAE for wheat (orange) or *Brassica* (purple) (B). Period and RAE were estimated by FFT NLLS, BAMP dtr, 24-120h cut-off. Wheat: 17°C (N=17/23); 22°C (N=32/32); 27°C (N=11/11); 32°C (N=15/15). *Brassica*: 12°C (N=24/24); 17°C (N=35/35); 22°C (N=30/30). An additional preliminary experiment consistent with these observations can be seen in Supplementary S13. Significance codes: ***p<0.001.

Figure 6. DF can be used to measure period differences between elite cultivars in *Brassica* and wheat. 10cm sections from the second leaf of 25 day old wheat seedlings were imaged under D:D at 27°C. 3cm square sections from the first leaf of 21 day old *Brassica* seedlings were imaged under L:L at 22°C. Period boxplots based on the DF oscillations from different cultivars are shown for wheat (A) and *Brassica* (B). The three replicates in the *Brassica* data represent different seed batches. Period values were estimated using FFT NLLS, BAMP dtr, 24-120h cut-off window. BAMP de-trended DF data was normalised to the mean DF intensity across all cultivars and plotted against time in hours after dawn (C and D). *Brassica* data represents results from two cabinets normalised for between-cabinet effects. Wheat data represents results from two identical experiments with two imaging cabinets run in parallel as technical replicates and normalised for the between-cabinet and experimental-run effects. Wheat: Robigus (N=25/25), Cadenza (N=12/12), Chinese Spring (N=24/25), Claire (N=27/27), Weebil (N=22/24), Paragon (N=24/4), Norin-61 (N=25/25). *Brassica*: for each seed batch of Cabriolet, Chuanyou II, Norin (N=8/8). *Brassica* data is consistent with previous experiments shown in supplementary materials S14. Significance codes: for wheat cultivars (A),***p<0.001, **p<0.01 relative to either *a*=Norin 61 or *b*=Paragon. For brassica cultivars (B), significantly different periods (p<0.05) are labelled relative to *a*=Norin Y1, *b*=Norin Y2 or *c*=Norin Y3.

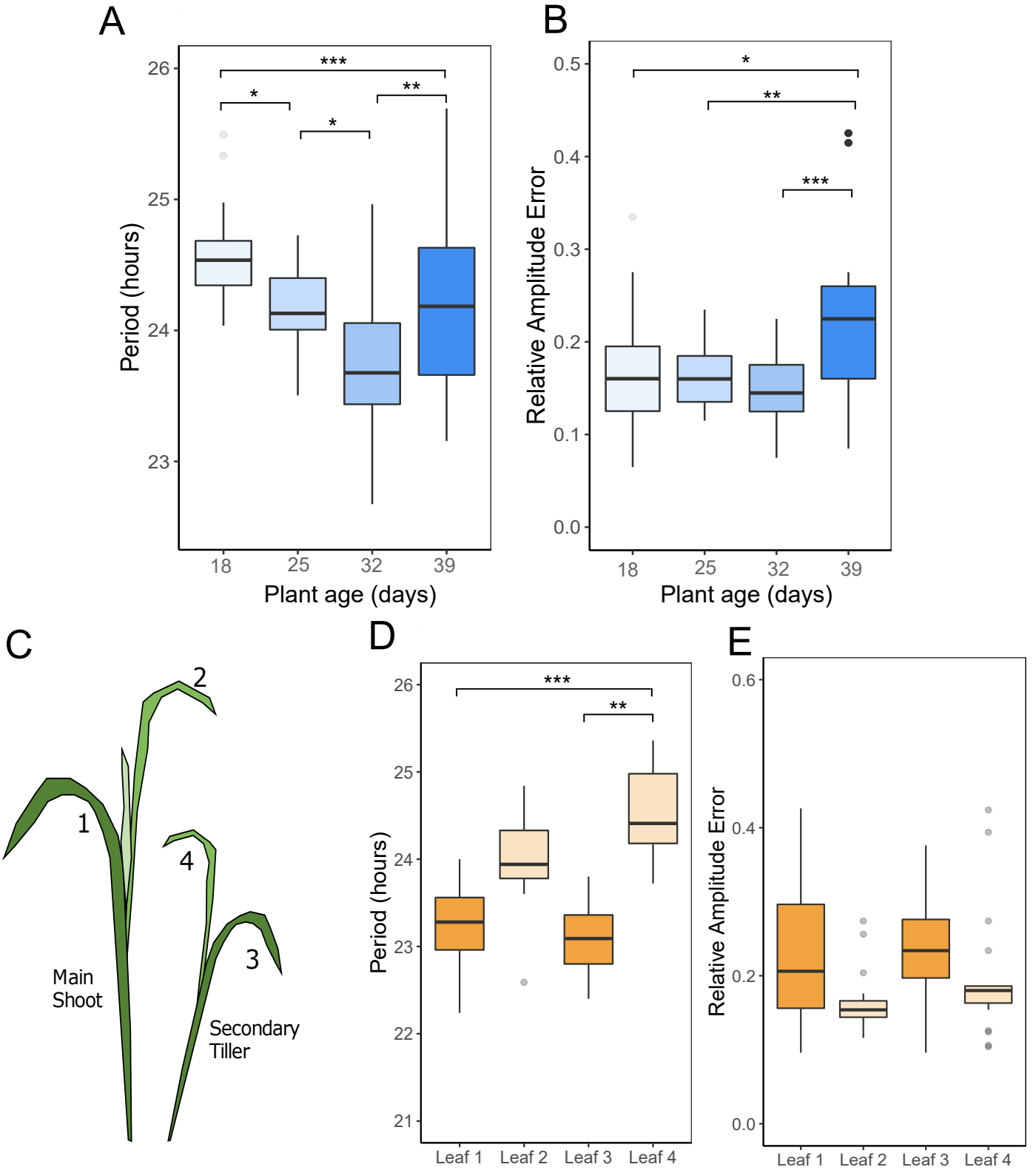
A
Period (hours)
26
25
24
23
***
*
**
*
18
25
32
39
Plant age (days)
B
Relative Amplitude Error
0.5
0.4
0.3
0.2
0.1
0.0
*
**
***
18
25
32
39
Plant age (days)
C
1
2
3
4
Main Shoot
Secondary Tiller
D
Period (hours)
26
25
24
23
22
21
***
**
Leaf 1
Leaf 2
Leaf 3
Leaf 4
E
Relative Amplitude Error
0.6
0.4
0.2
0.0
Leaf 1
Leaf 2
Leaf 3
Leaf 4

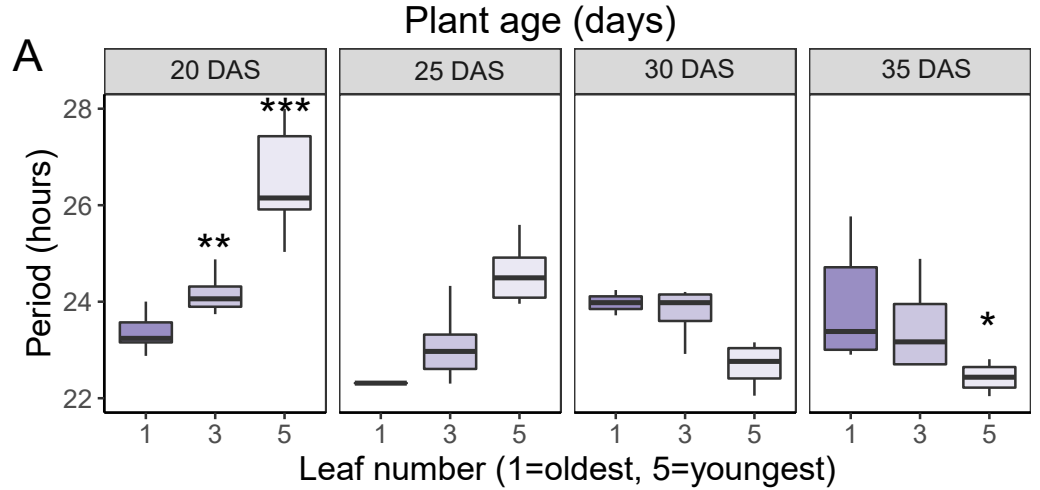
A
Plant age (days)
20 DAS
25 DAS
30 DAS
35 DAS
Period (hours)
28
26
24
22
***
**
*
1
3
5
Leaf number (1=oldest, 5=youngest)

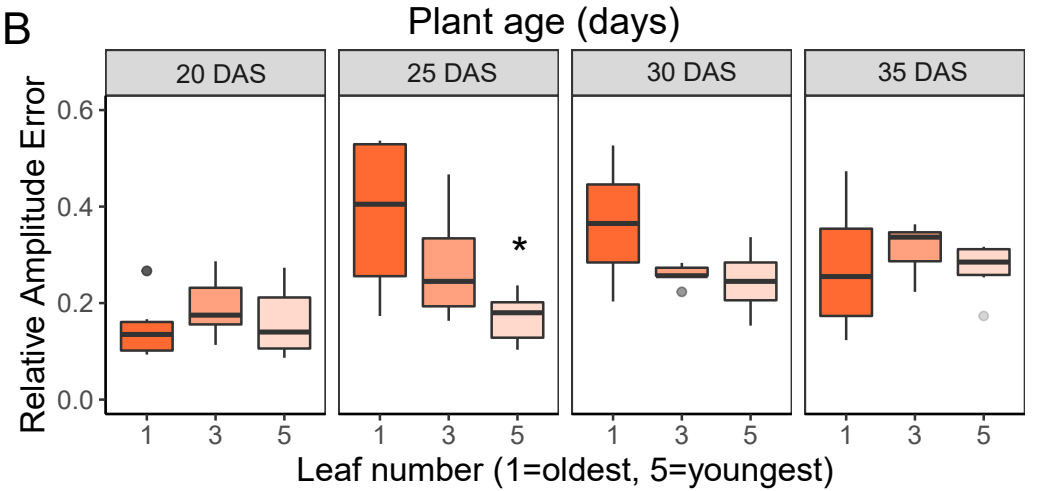
B
Plant age (days)
20 DAS
25 DAS
30 DAS
35 DAS
Relative Amplitude Error
0.6
0.4
0.2
0.0
*
1
3
5
Leaf number (1=oldest, 5=youngest)

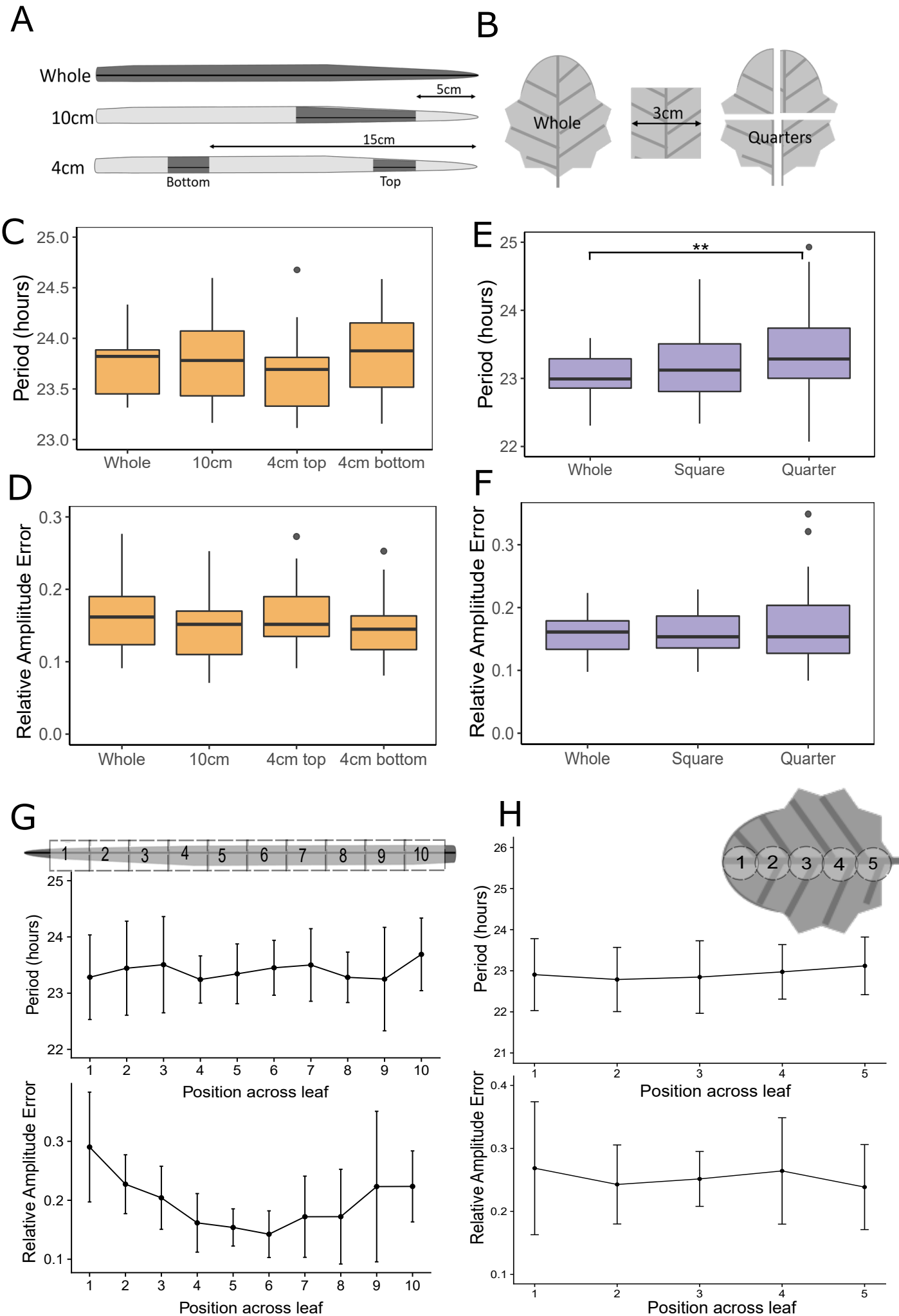
A
Whole
5cm
10cm
15cm
4cm
Bottom
Top
B
Whole
3cm
Quarters
C
Period (hours)
Whole
10cm
4cm top
4cm bottom
D
Relative Amplitude Error
Whole
10cm
4cm top
4cm bottom
E
Period (hours)
**
Whole
Square
Quarter
F
Relative Amplitude Error
Whole
Square
Quarter
G
Period (hours)
Position across leaf
Relative Amplitude Error
Position across leaf
H
Period (hours)
Position across leaf
Relative Amplitude Error
Position across leaf

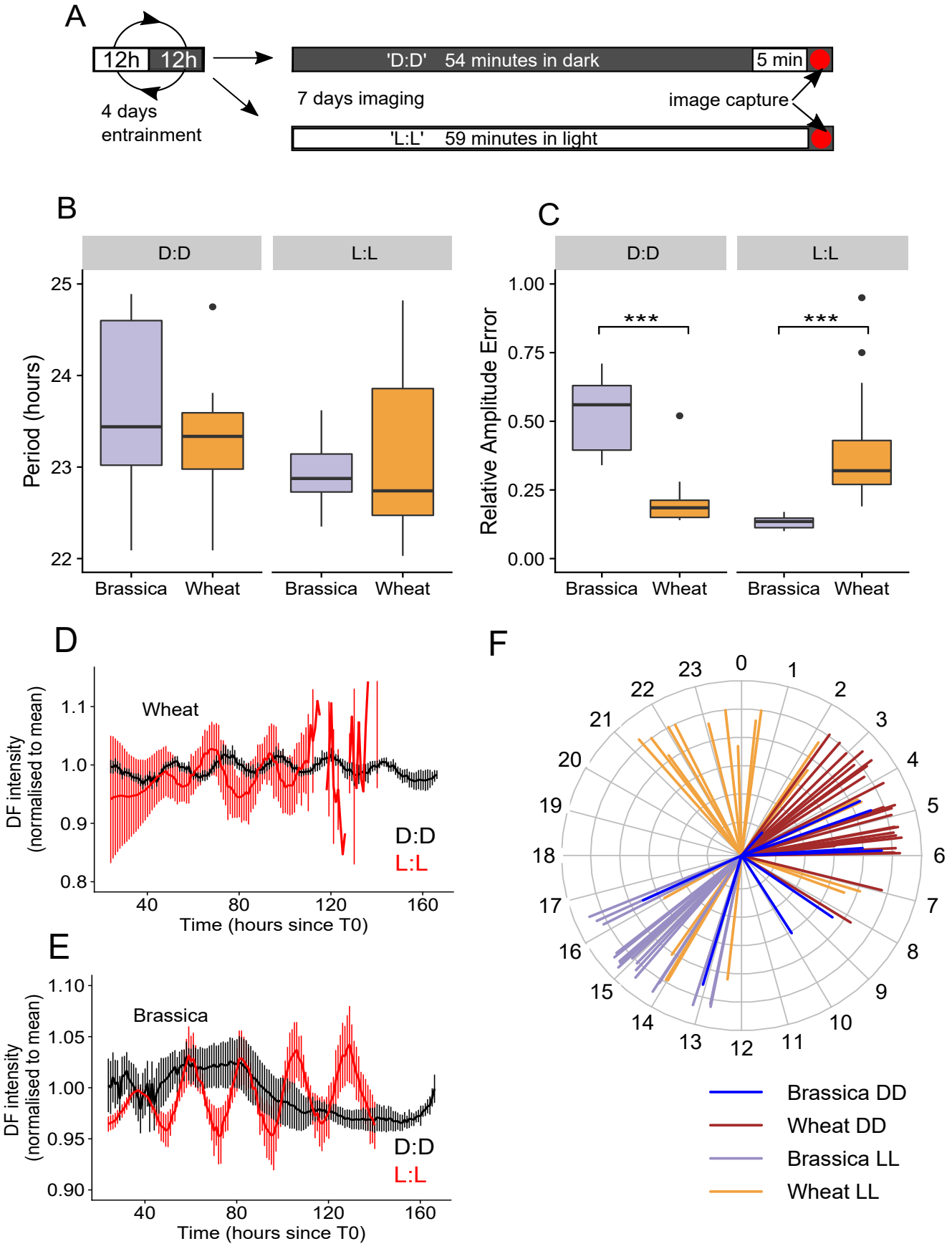
A
12h
12h
4 days
entrainment
'D:D' 54 minutes in dark
5 min
7 days imaging
image capture
'L:L' 59 minutes in light
B
D:D
L:L
Period (hours)
25
24
23
22
Brassica
Wheat
Brassica
Wheat
C
D:D
L:L
Relative Amplitude Error
1.00
0.75
0.50
0.25
0.00
***
***
Brassica
Wheat
Brassica
Wheat
D
Wheat
DF intensity
(normalised to mean)
1.1
1.0
0.9
0.8
D:D
L:L
40
80
120
160
Time (hours since T0)
E
Brassica
DF intensity
(normalised to mean)
1.10
1.05
1.00
0.95
0.90
D:D
L:L
40
80
120
160
Time (hours since T0)
F
0
1
2
3
4
5
6
7
8
9
10
11
12
13
14
15
16
17
18
19
20
21
22
23
Brassica DD
Wheat DD
Brassica LL
Wheat LL

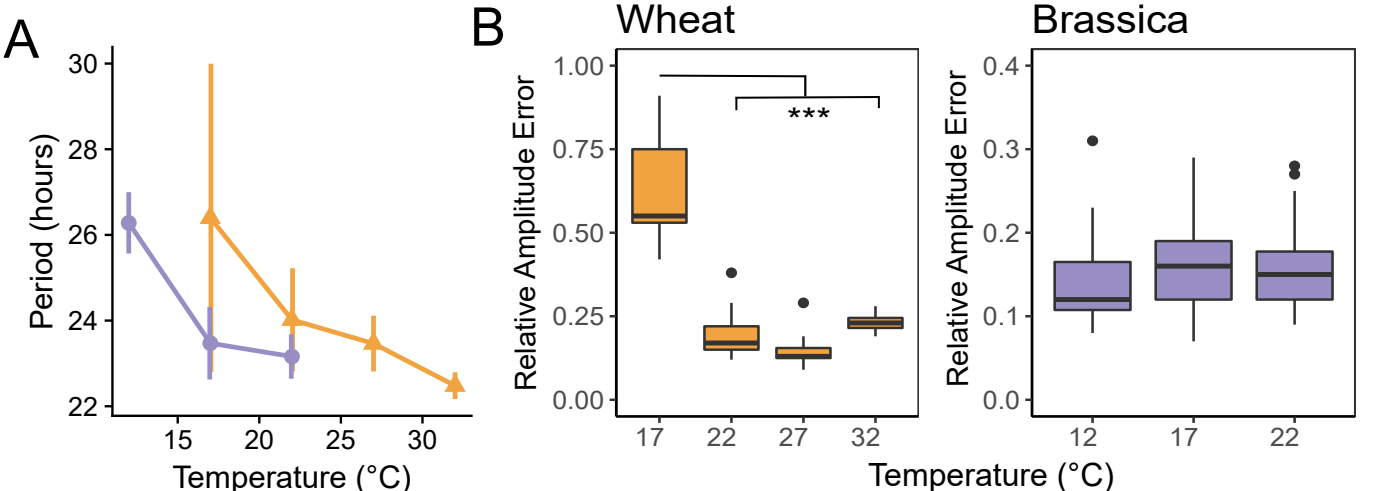
A
Period (hours)
30
28
26
24
22
15
20
25
30
Temperature (°C)
B
Wheat
Brassica
Relative Amplitude Error
1.00
0.75
0.50
0.25
0.00
***
17
22
27
32
Relative Amplitude Error
0.4
0.3
0.2
0.1
0.0
12
17
22
Temperature (°C)

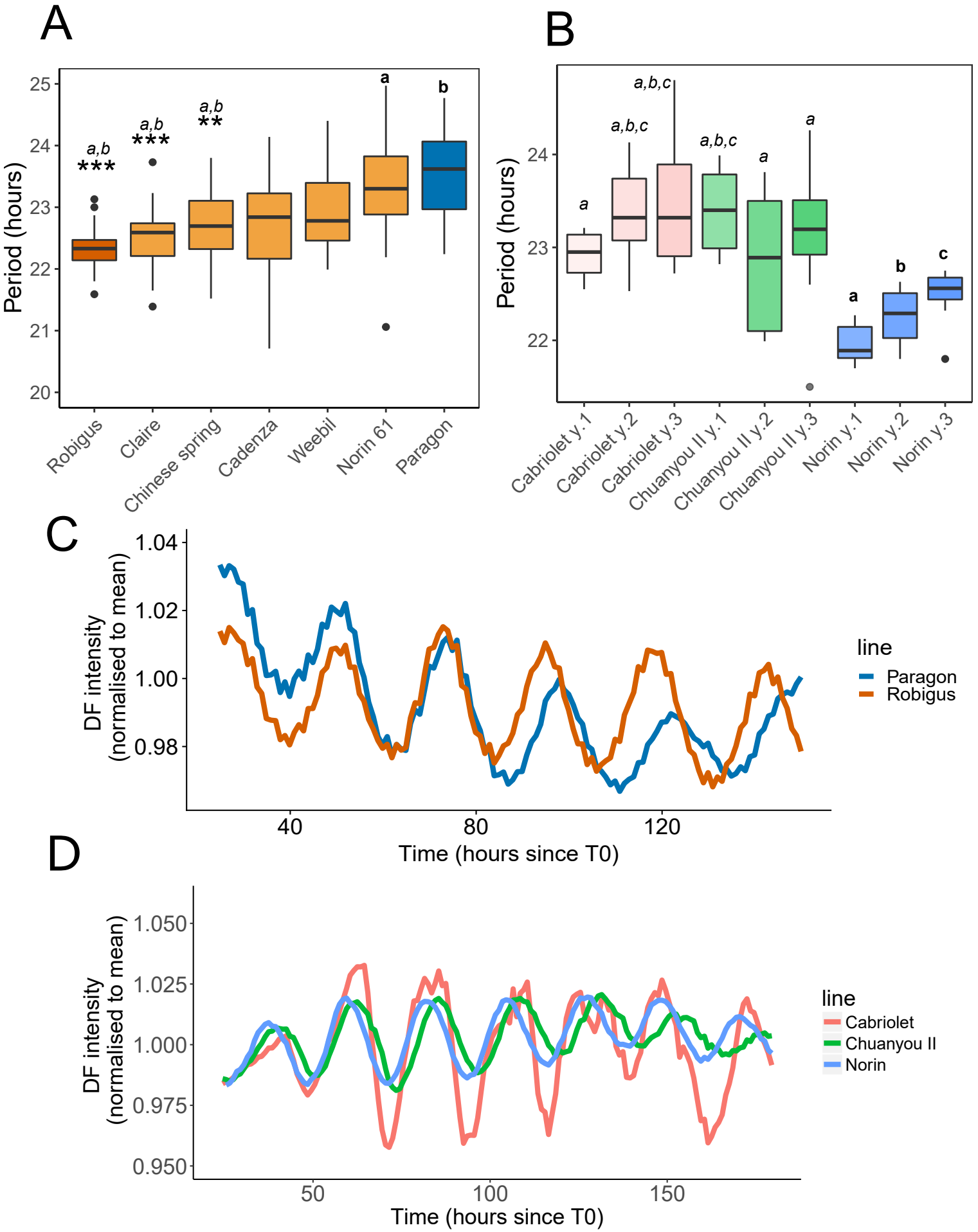
A
Period (hours)
25
24
23
22
21
20
a,b
***
a,b
***
a,b
**
a
b
Robigus
Claire
Chinese spring
Cadenza
Weebil
Norin 61
Paragon
B
Period (hours)
24
23
22
a
a,b,c
a,b,c
a,b,c
a
a
a
b
c
Cabriolet y.1
Cabriolet y.2
Cabriolet y.3
Chuanyou II y.1
Chuanyou II y.2
Chuanyou II y.3
Norin y.1
Norin y.2
Norin y.3
C
DF intensity
(normalised to mean)
1.04
1.02
1.00
0.98
40
80
120
Time (hours since T0)
line
Paragon
Robigus
D
DF intensity
(normalised to mean)
1.050
1.025
1.000
0.975
0.950
50
100
150
Time (hours since T0)
line
Cabriolet
Chuanyou II
Norin